Chapter 6
Using Molecular Beacons to Study Dispersal of mRNPs from the Gene Locus

Patrick T. C. van den Bogaard and Sanjay Tyagi

Keywords Molecular beacons; Single particle tracking; mRNA transport; Nuclear viscosity; Live-cell imaging

Abstract Before leaving the site of transcription, newborn messenger RNAs (mRNAs) become associated with a number of different proteins. How these large messenger ribonucleoprotein (mRNP) complexes then move through the dense nucleoplasm to reach the nuclear periphery has been a fascinating question for the last few years. We have studied the mechanism of this process by tracking individual mRNPs in real time. We were able to track mRNPs at single-molecule resolution because we utilized mRNAs that were engineered to have a sequence motif repeated 96 times in their untranslated region. These mRNAs were visualized with the help of molecular beacons that were specific for the repeated sequence; the binding of 96 molecular beacons to each mRNA molecule rendered them so intensely fluorescent that they were visible as fine fluorescent spots that could be tracked by high-speed video microscopy. In this chapter, we describe the details of the construction of genes containing the tandem repeats, the integration of such genes into the genome of a cell line, the design and testing of molecular beacons, time-lapse imaging of mRNPs, and computer-aided generation and analysis of the tracks of the individual mRNPs. These methods will be useful for studies of other dynamic processes such as mRNA export, splicing, and decay.

1 Introduction

The nuclei of cells of higher eukaryotes have a diameter of about 5 μm and yet they house DNA strands with cumulative length of 3 m or more. This large quantity of DNA is tightly associated with histones and other chromatin proteins. Even though the DNA exists in a highly organized state in the interphase nucleus, it creates a highly viscous environment. When mRNAs are produced at a gene locus they get immediately associated with a number proteins (as many as two dozen) that remain bound to them throughout their journey to the ribosomes in the cytoplasm. These

R. Hancock (ed.) *The Nucleus: Volume 2: Chromatin, Transcription, Envelope, Proteins, Dynamics, and Imaging*,

ribonucleoprotein complexes (RNPs) are much larger than the mRNA in terms of their mass. How these large complexes then travel to the nuclear pore through the dense chromatin has remained an unresolved question for the last few years ***(1)***. Assuming that the viscosity of the nucleus would be too high for the mRNP to overcome, early workers proposed that mRNPs are transferred along a chain of receptors until they reach a nuclear pore, expending metabolic energy in the process ***(2)***. This solid-state transport model is supported by observations that some mRNA transcripts are distributed along tracks that originate from the locus of the parent gene in fixed nuclei ***(3)***. According to an alternate theory called the gene-gating hypothesis, active genes would be situated near nuclear pores and mRNAs would exit the nucleus through the nearest pores ***(4)***. The gene-gating hypothesis is supported by observations that certain mRNAs exit from one side of the nucleus ***(5)*** and that, in yeast, many transcriptionally active gene loci are associated with nuclear pore proteins while quiescent loci, which are normally present near the center of the nucleus, move to the periphery upon induction ***(6)***. More recent studies indicate that simple Brownian diffusion is sufficient to account for mRNA transport within the nucleus ***(7, 8)***.

We have studied this issue by developing unique reporter genes and oligonucleotide probes that allow imaging and tracking of individual mRNPs in live cells ***(8)***. We utilize oligonucleotide probes called molecular beacons that become fluorescent upon hybridization ***(9)***. Molecular beacons are hairpin-shaped molecules with an internally quenched fluorophore whose fluorescence is restored when they bind to a target nucleic acid (Fig. 6.1).

The fluorescence of a target-bound molecular beacon is a hundred to a thousand times more intense than that of the free molecular beacon ***(9)***. Owing to their stem, the recognition of targets by molecular beacons is so specific that if the target differs even by a single nucleotide the probe does not bind to it. In order to ensure that the molecular beacons will be stable in the cell and that their hybrids will not be digested by ribonuclease H, the molecular beacons can be made from 2′-*O*-methylribonucleotides ***(10)***. Many different fluorophores can be utilized to detect

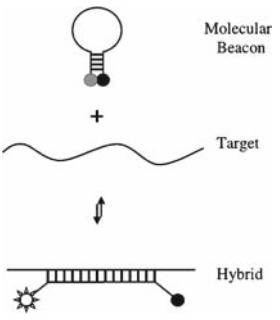

Fig. 6.1 Operation of molecular beacons. On their own, these molecules are nonfluorescent because the stem hybrid keeps the fluorophore close to the quencher. When the probe sequence in the loop hybridizes to its target, forming a rigid double helix, a conformational reorganization occurs that separates the quencher from the fluorophore and leads to an increase in fluorescence

several mRNAs in the same cell. The capacity of molecular beacons to recognize and report the presence of a specific mRNA in the complex cellular environment was demonstrated by imaging the distribution and following the localization process of native *oskar* mRNA from nurse cells to the posterior end of the fruit fly oocyte ***(11)***.

Since most genes produce just a few molecules of mRNA, it is desirable to be able to detect and track individual mRNA molecules. The fluorescence emitted by a single fluorophore, though detectable under specialized microscopic conditions, is too faint for tracking individual mRNPs. Since the monitoring of molecular motion requires high-speed video microscopy with exposure times around 100 msec, it is important to have a high fluorescence signal emanating from the target molecules. Therefore, we have developed an approach where multiple target sequences were incorporated in a relatively less important 3′-untranslated region of an mRNA ***(8)***. This multimeric target sequence could bind 96 copies of the same molecular beacon, rendering this mRNA so fluorescent that each individual molecule could be detected in the living cell as a diffraction-limited spot. The gene encoding a GFP-mRNA-96-mer was expressed in CHO cells and its mRNA was successfully tracked in the nucleus. Moreover, after export from the nucleus, the mRNAs could be clearly detected in the cytoplasm and their translation gave raise to green fluorescent protein (GFP) fluorescence, indicating that the molecular beacons bound to the mRNA did not hamper its nucleo–cytoplasmic export and subsequent translation.

So far, this approach has been utilized only for the exploration of mRNA dynamics within the nucleus but it should be effective for other contexts in which mRNA dynamics are studied. Other processes include mRNA splicing and maturation, mRNA export from the nucleus to the cytoplasm, mRNA localization in cytoplasm, and mRNA decay.

In this chapter, we describe procedures for making a gene encoding the tandem repeats, making a cell line in which this gene is integrated, design of molecular beacons that will be effective in mRNA imaging, delivery of molecular beacons into the cell, time-lapse imaging of individual mRNA molecule in living cells, and a computer algorithm to obtain and analyze single molecules tracks from the time lapse images.

2 Materials

2.1 Equipment

1. Spectrofluorometer (Photon Technology International, Birmingham, NJ, USA).
2. Spectrofluorometric thermal cycler: 7700 Prism (Applied Biosystems Foster City, CA, USA).
3. Microinjection apparatus (FemtoJet; Brinkmann, Westbury, NY, USA).

4. Inverted fluorescence microscope with heated stage and ×100 oil-immersion objective (Axiovert 200 M; Carl Zeiss MicroImaging, Thornwood, NY, USA).
5. CCD camera cooled to −30°C (CoolSNAP HQ; Photometrics, Tucson, AZ, USA) mounted on the bottom port of the microscope, with image acquisition software.
6. Open culture dish environmental control system with culture dishes coated with conductive material for controlled heating (Delta T4; Bioptechs, Butler, PA, USA).

2.2 Cells and Cell Culture

1. CHO–AA8-Tet-off cell line (Clontech, Mountain View, CA, USA).
2. Eagle's minimal essential medium supplemented with glutamine (Sigma-Aldrich, St. Louis, MO, USA) and 10% TET-System-Aproved FBS (Clontech).
3. Geneticin (G-418; Clontech).
4. Doxycycline (Clontech).

2.3 Plasmids and Cloning

1. Plasmid pGEM-11Zf(+) (Promega, Fitchburg Center, WI, USA).
2. Plasmid pTRE-d2EGFP (Clontech).
3. Competent cells: *Escherichia coli* MAX Efficiency Stbl2 (Invitrogen, Carlsbad, CA, USA).
4. Restriction enzymes.
5. Complementary DNA oligonucleotides for the repeat sequence (IDT, Coralville, IA, USA) (*see* **Section 3.1.2**).

2.4 Reagents and Solutions

1. Nuclease-free water (Ambion, Austin, TX, USA).
2. TE buffer: 1 m*M* EDTA, 10 m*M* Tris-HCl, pH 8.0.
3. Phosphate-buffered saline (PBS) with $CaCl_2$ and $MgCl_2$ (Sigma-Aldrich).
4. Molecular Beacon: dissolve molecular beacons for stock solutions in nuclease-free water and store at −20°C. Dilute working solutions in water, keep protected from light, and store at −20°C for up to 1 month. Filter through 0.2-μm filters to avoid clogging of needles. Wash the filters with the same water in which the probes are dissolved beforehand.
5. Oligonucleotide complementary to the molecular beacon: dissolve in TE and store at −20°C.

6. Full-length mRNA to be studied: transcribed in vitro from a plasmid (*see* **Section 3.2.2**).
7. Hybridization buffer: 1 m*M* $MgCl_2$, 20 m*M* Tris-HCl, pH 8.0.
8. Image processing software: MATLAB with the imaging-processing toolbox (MathWorks, Natick, MA, USA).

3 Methods

3.1 Construction of a Gene Encoding an mRNA with Tandem Repeats

3.1.1 Choosing the Sequence of Repeats

An important consideration for choosing the nucleotide sequence of the tandem repeats is that the molecular beacon target sequence in the repeat should be accessible to the probe and not occluded by secondary structure. It is possible to predict probe accessibility to some extent using the RNA-folding program m-fold (www.bioinfo.rpi.edu/applications/mfold) (*see* **Note 1** and **ref. (*12*)**). This algorithm presents the user with a number of thermodynamically favorable structures. In practice, none of the predicted individual secondary structures represents the true naturally occurring conformation; however, an analysis of all suboptimal structures is useful in identifying the probe-accessible sites. For that analysis, we look at the *ss-count* and *P-num* parameters to find probable molecular beacon binding targets. The *ss-count* describes the number of times a specific nucleotide is present in single-stranded form among all the predicted structures, while the *P-num* value counts the number of different base pairs that was found for that particular nucleotide when it was not single stranded. The repeated sequence should preferably have a high overall *ss-count* (>50%), since nucleotides with a low *ss-count* are strongly involved in base pairing. However, the *P-num* indicates if these nucleotides with low *ss-count* have a high stability (low *P-num*) or are unstable and not very consequential (high *P-num*). Since any arbitrary sequence can be chosen for the repeat unit, alter your sequence until it has almost no secondary structures. Then repeat the analysis with tandem concatemers of the sequence.

A second consideration in the selection of the repeat sequence is that it should be longer than the molecular beacon target site. If the molecular beacon probe sequence is the same length as the repeat sequence, the fluorophore of each molecular beacon will be quenched by the quencher of the molecular beacon bound at the neighboring site. In order to overcome this problem, we make the repeat unit at least 10 nucleotides (nt) longer than the target. The spacer of 10 nt that this strategy provides places the fluorophore more than 100 Å apart from the quencher, a distance beyond which there is no significant fluorescence resonance energy transfer.

A further consideration is that one arm of the molecular beacon is made to bind the target so that the arms of neighbor molecular beacons do not bind to each other. Below we will describe the construction of the multimer used for the study of mRNA transport in the nucleus as an example ***(8)***.

3.1.2 Cloning Tandem Repeats

As an example, we describe the cloning of 96 repeats of the 50-nt-long sequence 5′-CAGGAGTTGTGTTTGTGGACGAAGAGCACCAGCCAGCTGATCGACCT CGA-3′ used in our studies of mRNP diffusion ***(8)***. As a repeating unit, this multimer has an overall high *ss-count* as well as a high *P-num* per nucleotide, indicating that many different secondary structures are predicted (*mfold*) but none of them are considered stable. The construction of the direct repeats was carried out by the procedure described previously by Robinett et al. ***(13)***. In this procedure, a synthetic DNA insert corresponding to one element of the array is cloned into a plasmid. This insert is then excised and reinserted at the tail end of the monomeric insert, producing a clone containing a dimeric insert. This cycle is repeated with the dimeric clone to obtain a tetrameric insert, and then the cycle is repeated again to obtain the desired length of the insert, which doubles in each cycle.

In our implementation, the repeat sequence contained an *Sal*I site on its 5′ terminus and an *Xho*I and *Bam*HI site respectively on its 3′ terminus (Fig. 6.2).

The procedure relied on the fact that the restriction enzymes *Sal*I and *Xho*I generate overhangs that are compatible with each other, however, the product of ligation cannot be cut again by the same enzymes (*see* **Note 2**). Two strands for the repeat sequence (*see* **Section 2.3.5**) were ordered separately and annealed together to form a double-stranded DNA. The sequences of the strands are TCGACAGGA GTTGTGTTTGTGGACGAAGAGCACCAGCCAGCTG ACTCGAGCCGAGG and GATCCCTCGGCTCGAGTCAGCTGGCTGGTGCTCTTCGTCCACAAAC ACAACTCCTG. The annealed strands were phosphorylated, which resulted in a double-stranded fragment with *Sal*I and *Bam*HI overhangs and an internal *Xho*I site. The vector pGEM-11 was digested with *Sal*I and *Bam*HI and ligated with this synthetic insert. The integrity of the resulting construct (pGEM-1×) was verified by restriction analysis with *Sal*I and *Bam*HI. Due to its small size, the presence of the insert was confirmed by electrophoresis on a 10% polyacrylamide gel against a 100-bp marker.

For dimerization of the insert, a monomeric *Sal*I and *Bam*HI fragment obtained by digestion of pGEM-1× was inserted in the same plasmid digested with *Xho*I and *Bam*HI, yielding pGEM-2×. To create the tetramer repeat, a portion of pGEM-2× was digested with *Sal*I and *Bam*HI and the dimer insert was ligated into the vector fragment (containing the dimer) of another portion of pGEM-2× that was digested with *Xho*I and *Bam*HI, yielding pGEM-4×. Repeating these steps led ultimately to vectors containing a 32-mer and a 64-mer repeat (pGEM-32× and pGEM-64×). In the same way as described above, these two vectors were used to create pGEM-96×. During these cloning steps, special host cells that minimize recombination (MAX Efficiency

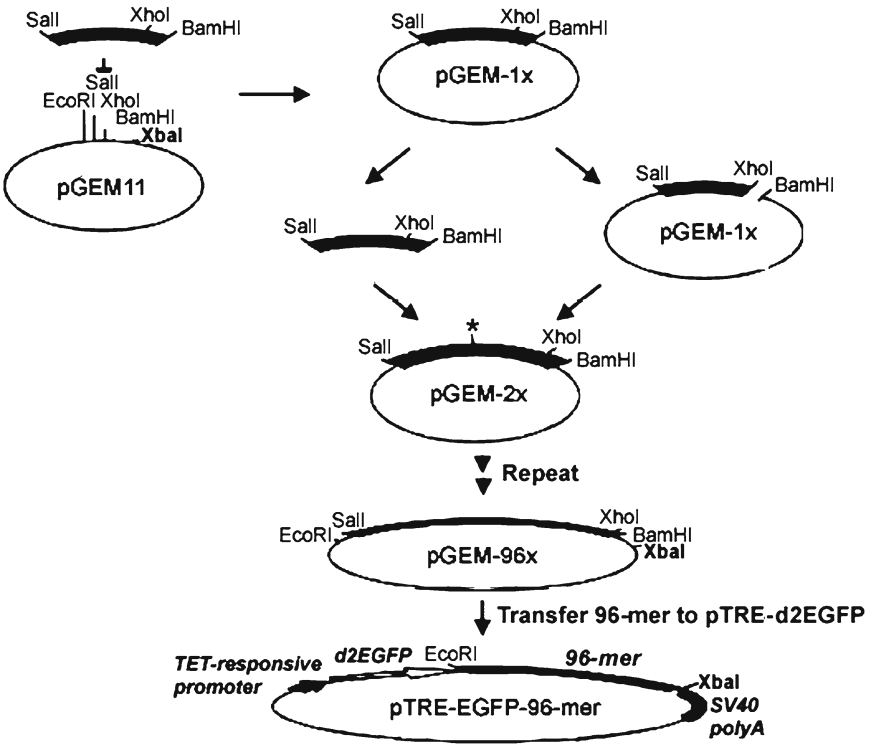

Fig. 6.2 Assembly of the reporter gene with multimeric repeats. After annealing both strands, the basic unit is inserted into pGEM11 digested with restriction enzymes *Sal*I and *Bam*HI, resulting in the vector pGEM-1×. The principle of forming the multimeric repeats is to ligate the new unit digested with *Sal*I and *Bam*HI into the same vector digested with *Xho*I and *Bam*HI, and then to repeat the cloning cycle again until the desired number of repeats is obtained

Stbl2 competent cells) were used to reduce the tendency to deletions and rearrangements of the multimer and that were exclusively grown at 30°C.

The pTRE-GFP-96-mer was created by excision of the 96-mer from pGEM-96× with *Eco*RI and *Xba*I and ligation into pTRE-d2EGFP digested with the same enzymes. Since long tandem repeats are not well tolerated by the host cells, in order to make a preparation of plasmids containing 32 or more repeats, we grow many pure colonies in broth and utilize only those that have maintained the full-length insert.

pTRE-GFP-96-mer was used to transfect the CHO-AA8-Tet-off cell line that contains a stably integrated gene for the tetracycline-controlled Tet-off transactivator. A geneticin (G-418)-resistant clone (CHO-GFP-96-mer) was selected based on GFP expression in the absence of doxycycline. This clone did not express GFP in presence of doxycycline (10 ng/mL).

3.2 Molecular Beacons

3.2.1 Design

For live cell imaging, we normally use molecular beacons with a 2′-O-methyl backbone as these are resistant to cellular nucleases, and their hybrids with RNA are not degraded by ribonuclease H. However, this change in the backbone alters the thermodynamic characteristics of the probe; both the probe–target hybrid and the stem hybrids become stronger (melting at higher temperatures). While the former does not cause any problems, the latter results in probes that have difficulty opening in response to the target so that the kinetics of probe–target hybridization become sluggish. To overcome this problem, a smaller (4–5 nt) and/or less G/C-rich sequence can be chosen for the stem. The length of the probe sequence in the molecular beacon should be such that the probe–target hybrid melts at 7–10°C higher than the detection temperature (usually 37°C). A length of 15–25 nt is usually chosen for the probe loop. The molecular beacon should not have any tendency to fold into any other structure besides the designed stem–loop; this can be predicted using the DNA folding program available at http://www.bioinfo.rpi.edu/applications/mfold/cgi-bin/dna-form1.cgi. The sequence of the molecular beacon used for our example was Cy-3-5′-CUUCGUCCACAAACACAACUCCUGAAG-3′-Black Hole Quencher 2.

3.2.2 Testing the Molecular Beacon

The molecular beacon preparation should be purified using high-pressure liquid chromatography and should not contain any free fluorophores or any oligonucleotide fragments containing the fluorophore but without a quencher. Molecular beacons can be functionally tested in a fluorometer by measuring the change in their fluorescence after adding the complementary oligonucleotide (*see* **Note 3**). Preparations that have at least 30 times more fluorescence in their target-bound state then in their free state are considered good. The thermodynamic characteristics of the molecular beacons are obtained by measuring the denaturing profile in a real-time PCR instrument (*see* **Note 4**). The melting temperature of the probe–target hybrids should be at least 7–10°C higher then the detection temperature (usually 37°C). Finally, the molecular beacons should be tested against full-length target mRNA that is prepared by transcribing a plasmid template in vitro (*see* **Note 5**).

3.3 Cell Culture and Image Acquisition

Despite the amplification of signals afforded by multimeric target sites, the signals from the individual mRNA molecules are rather faint and microscopy conditions are therefore optimized for low-light imaging. Among the steps that we take are: replace normal culture media with phenol-red free media before imaging; use thin

glass-bottom culture dishes; use a CCD camera cooled to −30°C; mount the camera on the bottom port of the microscope to avoid light paths with multiple glass elements; and use ×100 oil immersion objectives with high numerical apertures. Since we microinject the probes into cells, we use culture dishes that are open and have appropriate dimensions for access to the microinjection set-up. Furthermore, the temperature of the cells is maintained by controlled heating of the culture dish (T4 culture dishes are coated with conductive material for controlled heating) and the objective.

CHO-GFP-96-mer cells were grown in T4 glass culture dishes in the presence of doxycycline (*see* **Note 6**). For imaging, the culture dishes were placed on the inverted fluorescence microscope with heated stage and ×100 oil-immersion objective. The molecular beacons were dissolved in water at a concentration of 2.5 ng/μL, and a volume of 0.1 to 1 fL was injected into the cells (*see* **Note 7**). Removing the doxycycline from the growth medium started the expression of the GFP-mRNA-96-mer, and usually a bright fluorescent spot appeared in the nuclei between 60 and 90 min after induction. This spot represented the site of transcription, and was actually made up of multiple mRNA molecules and was therefore brighter that the intensity of individual mRNP particles. After this period, individual mRNA molecules were observed as diffraction-limited spots that emanated from the transcription site and distributed uniformly within the volume of the nucleus. Over time, the RNA molecules were found in the cytoplasm where they were functionally translated into GFP.

The exposure time and the time between successive image frames depends on the process that one wishes to follow. To characterize the diffusion of mRNP particles in the nucleus, the exposure time was set to 0.3 sec without any time between successive frames. To achieve higher intensities for the particles in these experiments, the images were recorded at 2× binning.

To study the behavior of the mRNP particles in relation to the chromatin density, heterologous histone H2B fused to GFP was expressed in the CHO cells. The fluorescence intensity of the GFP-H2B directly reflected the density of the chromatin into which it was incorporated ***(14)***. This visualization was possible because the simultaneous signal from the destabilized GFP from the reporter RNA was much lower in intensity and was localized in the cytoplasm.

3.4 Tracking Single mRNA Molecules

The mRNP particles were tracked by using custom software developed in MATLAB with its image processing toolbox. The images in a time series were first passed through a median filter, after which they were run through the custom linear filter, which was loosely based on the discrete Laplacian and specifically enhanced diffraction limited spots from their background. We have shown that each spot corresponds to an individual mRNA molecule, thus establishing that the method is a valid way to count the number of mRNA molecules in individual cells ***(8)***.

These particles were visually identified in the first frame, after which a local threshold was applied to reveal each particle's outline. The centroid of each outline was used as that particle's position. Its position in subsequent frames was determined with the aid of a nearest maximum algorithm. If the algorithm failed to correctly identify a particle in the subsequent frame, then provision was made for manual identification. The precision of the particle's location was higher than the limit of optical resolution, because the center of a circle with fuzzy boundaries can be located with greater precision than the circle itself. Tracking was stopped if two particles came so close to each other that their identities became confused.

Among the possible types of movements are free diffusion caused by Brownian motion, corralled diffusion within a confined space, directed motion by external agents such as motor proteins, or no movement. All of these motion types are described by the relationship between the magnitude of displacement (MSD) of a particle and the time interval (*see* **Note 8**). We tracked the movement of single mRNAs in the nucleus and calculated their MSD by averaging the squares of all displacements of the particle between frames separated by a given time interval (Fig. 6.3). Furthermore, tracking also allowed us to calculate the diffusion constants for particles showing Brownian motion, the confines for corralled particles, and the speed of potentially directed movement.

The majority of the GFP-mRNA-96-mer particles displayed a linear relationship between the MSD and the time interval, with an average value of their diffusion constant of 0.033 $\mu m^2/s$. However, on average, about half of the mRNP particles were mobile at any moment while the other half were found to be stationary (apparent diffusion constant 0.0006 $\mu m^2/s$). When the tracks of all mRNP particles in one imaging plane of one nucleus were merged with the chromatin density image, it was clear that regions of low chromatin density were frequently visited by mobile

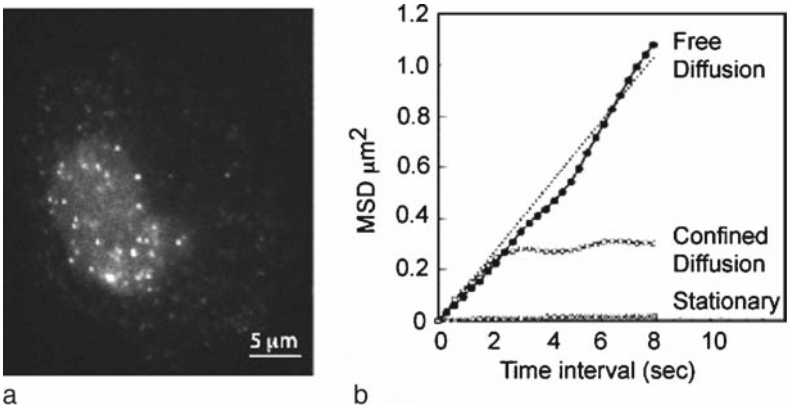

Fig. 6.3 Relationship the MSD of individual mRNP particles and the time interval of their displacement. **a** Typical frame of a time-lapse movie showing bright mRNP particles in the nucleus. **b** Examples are shown of three different types of movements displayed by the particles. The *dotted line* indicates the behavior of the majority of freely diffusing particles (average diffusion constant of 0.033 $\mu m^2/s$)

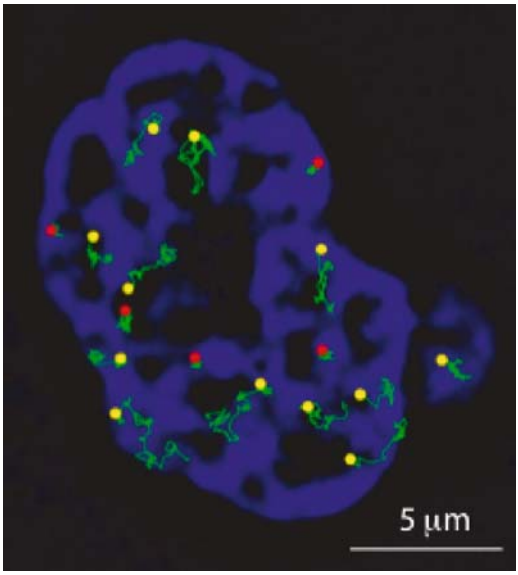

Fig. 6.4 Tracks of a few of the mRNP particles in a nucleus overlaid on an image of chromatin density. In *blue*, the fluorescence intensity of GFP-H2B directly reflected the density of the chromatin. The tracks are displayed in *green*, the final positions of mobile particles are shown by *green dots*, and those of stationary particles by *red dots.* To view this figure in color, see COLOR PLATE 4

particles while the stationary particles were found in the high-density chromatin (Fig. 6.4). Nucleoli were never visited by the mRNP particles. Interestingly, the diffusion constants of mobile particles were not strongly affected by factors like ATP depletion or lowered temperature, suggesting that the motion of these particles was not controlled by enzymatic processes. These factors did increase the fraction of stalled particles. This, together with the observation of stalled particles resuming a mobile state, suggests that the transition of a particle to assume the mobile state from the stalled state is an ATP-dependent process.

4 Notes

1. In the default settings of *m-fold*, the RNA is folded at 37°C. After folding, the individual secondary structures and their thermodynamic details are presented for viewing. The *ss-count* and *P-nums* for all the structures are presented in separate files and their data can be imported into a spreadsheet program like Microsoft Excel. This program outputs folding results for short sequences (up to 800 nt) immediately; however, for long RNAs you need to submit the job and retrieve the results later from the host server.
2. In this case, the combination of *Sal*I and *Xho*I was chosen; when their compatible cohesive ends are ligated, the resulting site is not recleavable by either enzyme. Other combinations of restriction enzymes are also possible for the same purpose, for example *Bcl*I/*Bam*HI, *Bgl*II/*Bam*HI, *Nsi*I/*Pst*I, or *Xba*I/*Spe*I to suit your own cloning needs.

3. Signal-to-background ratios of molecular beacons are tested in a spectrofluorometer using wavelengths of excitation and emission specific for the fluorophores. First measure the signal of 125 µL of the hybridization buffer (F_{buffer}). After 10 µL of a 0.5 µ*M* molecular beacon solution is added, a new fluorescence reading is taken (F_{closed}). Next, a fivefold molar excess of oligonucleotide target is added and the increase in fluorescence is recorded over time. When the maximum fluorescence is achieved (all molecular beacons have bound a target; F_{open}) the signal-to-background ratio is calculated as follows: $(F_{open} - F_{buffer}) / (F_{closed} - F_{buffer})$.
4. Thermal denaturation profiles of molecular beacons are measured in a spectrofluorometric thermal cycler using wavelengths of excitation and emission specific for the fluorophore. Add 50–100 ng of molecular beacon to the hybridization mix in a PCR tube, with and without a fivefold molar excess of oligonucleotide target. Decrease the temperature from 95°C to 25°C in steps of 1°C. To allow the equilibrium to form, hold each step for at least 30 sec. The denaturation profiles of the probes alone and with their oligonucleotide target should indicate correct molecular beacon characteristics (www.molecular-beacons.com).
5. Prepare in vitro-transcribed RNA from a linearized plasmid template using standard procedures. Add 10 µL of a 0.5 µ*M* solution of the molecular beacon to 125 µL of hybridization solution and measure fluorescence until the signal is stable. Add 10 µL of 100 n*M* in vitro-transcribed RNA and measure the increase in fluorescence intensity of the molecular beacon in a spectrofluorometer using wavelengths of excitation and emission specific for the fluorophore at 37°C.
6. The CHO Tet-off cells were regularly cultured at 37°C in the α modification of Eagle's minimal essential medium supplemented with glutamine, 10% TET-System-Approved FBS (*see* **Section 2.2.2**), and doxycycline (10 ng/mL). After injection with molecular beacons, the doxycycline was removed to allow expression. During this time, the cells were placed back in the incubator to keep them healthy before imaging commenced. The volume of imaging medium was kept large to buffer changes in temperature and CO_2 concentration.
7. Like all small oligonucleotides, molecular beacons are transported to the nucleus within minutes of their introduction into living cells ***(15)***. Because the free probes reside in the nucleus, the other cell compartments are free of background fluorescence that may be associated with molecular beacons in living cells.
8. The time intervals ranged from the time elapsed between two successive frames to the full duration of the time series. In the averaging, all pairs of time points were considered rather than just independent pairs. Only MSD measurements determined from time intervals shorter than 25% of the length of time during which each particle was tracked were used to calculate the particle's diffusion constant, because statistical variations became so large for longer intervals that artifactual corrals were predicted to be present where none existed. The diffusion constant of corralled particles (identified by the leveling off of their MSD at longer time intervals) was determined in the same manner, but only from data obtained during the shorter intervals in which they diffused freely. The average diffusion constants determined for each condition were computed by taking the weighted average of the diffusion constants for each particle track, where the

weight of each track was proportional to its length because longer tracks yielded statistically more significant data. Whereas this weighting may introduce a bias in the determination of the average diffusion constant in that less mobile particles are more likely to be able to be followed for longer periods, it also minimizes the influence of measurements made on particles whose movements are more difficult to resolve. Although the magnitude of the standard deviations of these measurements was similar to the magnitude of the diffusion constants, wide variations in diffusion constants are natural features of single-particle tracking measurements due to the stochastic nature of diffusion as well as to differences in the microenvironments through which the particles move.

Acknowledgments We thank Diana Y. Vargas and Arjun Raj for their contributions. This work was supported by the National Institutes of Health Grant GM-070357.

References

1. Politz, J. C. and Pederson, T. (2000) Movement of mRNA from transcription site to nuclear pores. *J. Struct. Biol*. **129**, 252–257.
2. Agutter, P. S. (1994) Models for solid-state transport: messenger RNA movement from nucleus to cytoplasm. *Cell Biol. Int*. **18**, 849–858.
3. Lawrence, J. B., Singer, R. H., and Marselle, L. M. 1989 Highly localized tracks of specific transcripts within interphase nuclei visualized by in situ hybridization. *Cell*. **57**, 493–502.
4. Blobel, G. (1985) Gene gating: a hypothesis. *Proc. Natl. Acad. Sci. USA*. **82**, 8527–8529.
5. Colon-Ramos, D. A., Salisbury, J. L., Sanders, M. A., Shenoy, S. M., Singer, R. H., and Garcia-Blanco, M. A. (2003) Asymmetric distribution of nuclear pore complexes and the cytoplasmic localization of beta2-tubulin mRNA in Chlamydomonas reinhardtii. *Dev. Cell*. **4**, 941–952.
6. Casolari, J. M., Brown, C. R., Komili, S., West, J., Hieronymus, H., and Silver, P. A. (2004) Genome-wide localization of the nuclear transport machinery couples transcriptional status and nuclear organization. *Cell* **117**, 427–439.
7. Shav-Tal, Y., Darzacq, X., Shenoy, S. M., Fusco, D., Janicki, S. M., Spector, D. L., and Singer, R. H. (2004) Dynamics of single mRNPs in nuclei of living cells. *Science*. **304**, 1797–1800.
8. Vargas, D. Y., Raj, A., Marras,. S. A., Kramer, F. R., and Tyagi, S. (2005) Mechanism of mRNA transport in the nucleus. *Proc. Natl. Acad. Sci. USA* **102**, 17008–17013.
9. Tyagi S, Bratu, D. P., and Kramer, F. R. (1998) Multicolor molecular beacons for allele discrimination. *Nat. Biotechnol*. **16**, 49–53.
10. Tsourkas, A., Behlke, M. A., and Bao, G. (2003) Hybridization of 2′-O-methyl and 2′-deoxy molecular beacons to RNA and DNA targets. *Nucleic Acids Res*. **31**, 5168–5174.
11. Bratu, D. P. Cha, B. J., Mhlanga, M. M., Kramer, F. R., and Tyagi, S. (2003) Visualizing the distribution and transport of mRNA in living cells. *Proc. Natl. Acad. Sci. USA* **100**, 13308–13313.
12. Zucker, M. (2003) Mfold web server for nucleic acid folding and hybridization prediction. *Nucleic Acids Res*. **31**, 1–10.
13. Robinett, C. C., Straight, A., Li, G., Willhelm, C., Sudlow, G., Murray, A., and Belmont, A. S. (1996) In vivo localization of DNA sequences and visualization of large-scale chromatin organization using lac operator/repressor recognition. *J. Cell Biol*. **135**, 1685–1700.
14. Kanda, T., Sullivan, K. F., and Wahl, G. M. (1998) Histone-GFP fusion protein enables sensitive analysis of chromosome dynamics in living mammalian cells. *Curr. Biol*. **26**, 377–385.
15. Tyagi, S. and Alsmadi, O. (2004) Imaging native β-actin mRNA in motile fibroblasts. *Biophys. J*. **87**, 4153–4162.